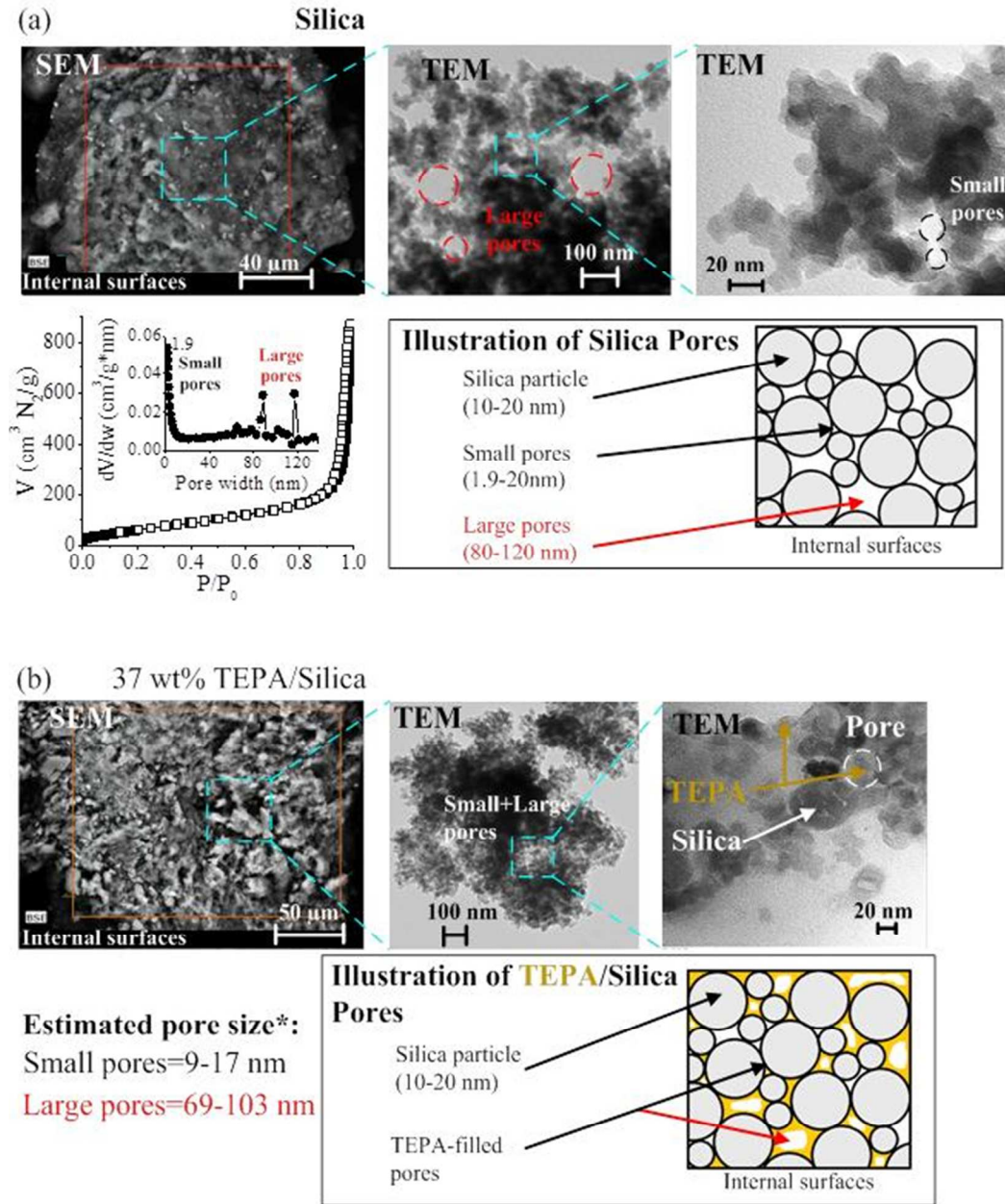


Supporting Information

Figures for Adsorption-Desorption Studies on TEPA/Silica Sorbents



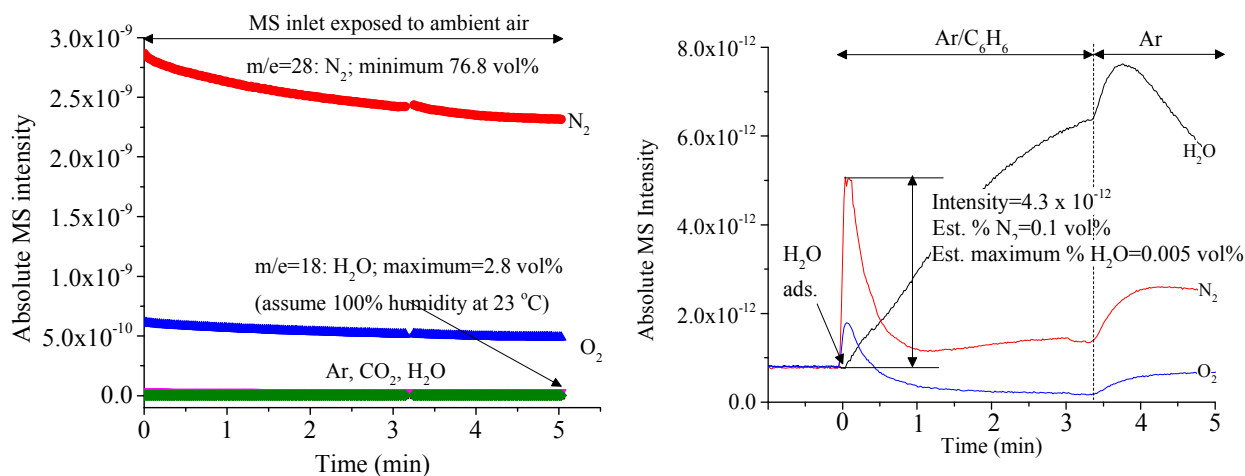


Figure S2. MS profiles of (a) ambient air and (b) N_2 , O_2 , and H_2O during benzene adsorption on silica at $40\text{ }^\circ\text{C}$.

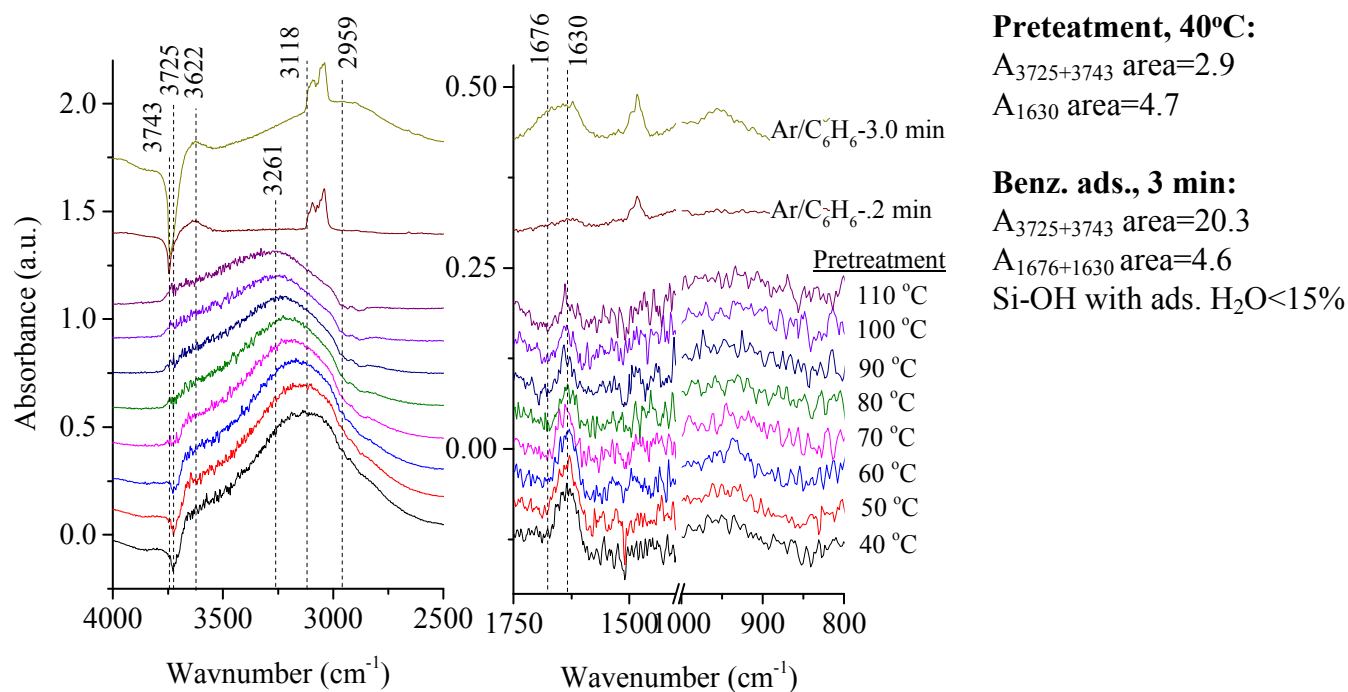


Figure S3. IR absorbance spectra of H_2O adsorbed on silica at different temperatures during pretreatment. The spectra were obtained by $\text{abs} = \log(I_{\text{cooling}}/I_{\text{heating}})$, where I_{heating} is the single beam spectrum of silica (contains ambient adsorbed H_2O) at different temperatures during heating to $110\text{ }^\circ\text{C}$ in $150\text{ cm}^3/\text{min}$ Ar flow and I_{cooling} is the corresponding single beam spectrum of silica at the same temperature during cooling.

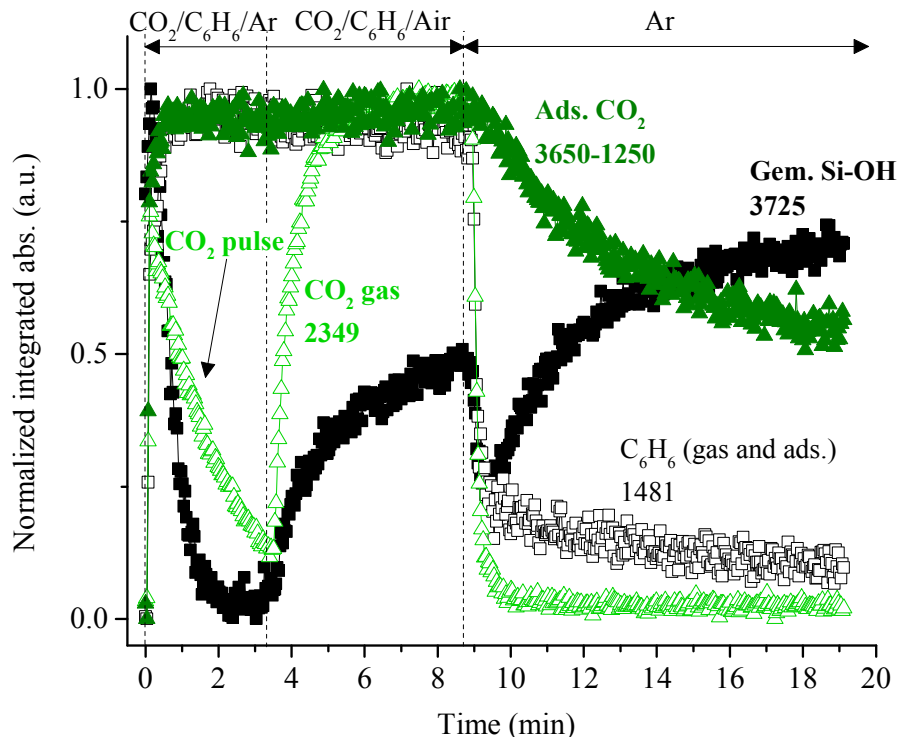


Figure S4. Complete IR integrated absorbance profiles during CO₂/benzene adsorption onto and desorption from 37 wt% TEPA/Silica

Results and Discussion for Benzene and Benzene/CO₂ Adsorption-Desorption of PEI/Silica

Additional benzene and benzene/CO₂ adsorption-desorption studies were performed on 36 wt% and 12 wt% polyethyleneimine (branched PEI, Mw=750,000)/Silica sorbents to further check the validity of probing the CO₂ adsorption/desorption process with adsorbed benzene. The EDS N mapping on the PEI sorbent particles is presented in Figure S5 and shows higher amine density on the internal surfaces, i.e. inside the pores, than external surface. This is in contrast to TEPA/Silica sorbents which show higher density on the external surface. The N/Si ratios of PEI/Silica are summarized in Table S1.

Table S1 shows that the sorbents with the same amine loading of PEI/Silica and TEPA/Silica have similar values in the intensity of Iso. (isolated) Si-OH, Gem. (geminal) Si-OH, and the sum

of these two intensities (Iso + Gem.). These values indicate the sorbents with the same level of amine loading possessed approximately same quantities of available Si-OH groups on the sorbents to adsorb benzene.

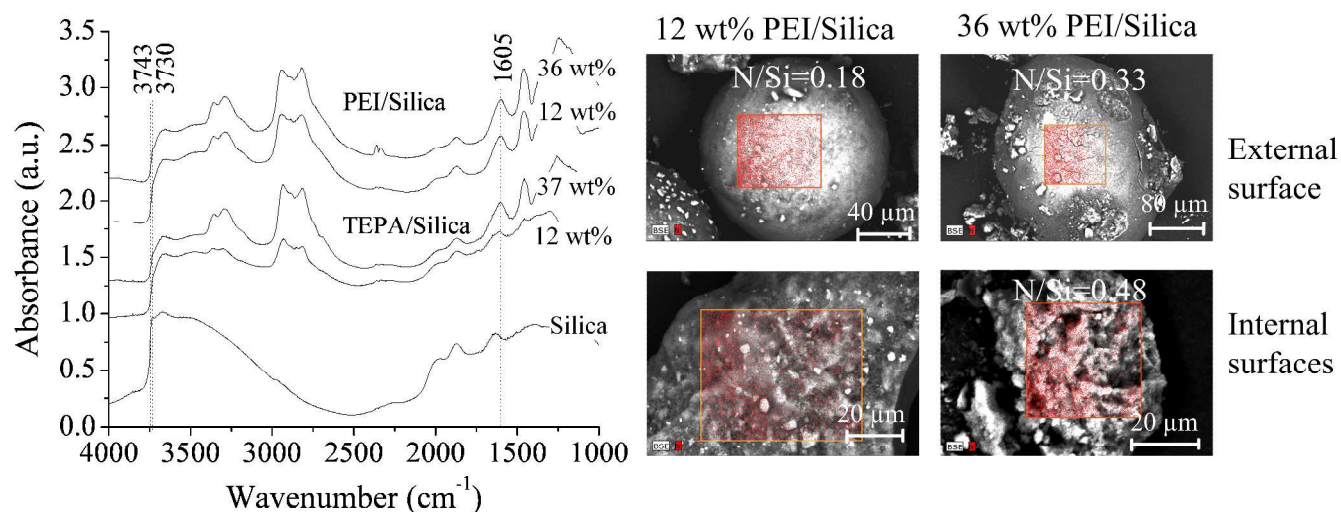


Figure S5. IR absorbance spectra ($\log(1/I)$) of fresh TEPA/Silica and PEI/Silica sorbents, and EDS N mapping on PEI/Silica.

Table S1: IR absorbance intensities, integrated absorbances, and EDS results for silica and the amine sorbents.

Sorbent	Fresh sorb. (abs. int. [$\log(1/I)$])			Benz.-ads. (integ. abs.)	N/Si ratio (EDS)	
	Iso. Si-OH	Gem. Si-OH	Iso.+Gem.	Iso. or Gem.	Int. surface	Ext. surface
Silica	0.66	0.78	1.44	20.5	0.06	0.07
12 wt% TEPA/Silica	0.17	0.31	0.48	5.8	0.17	0.24
37 wt% TEPA/Silica	0.1	0.22	0.32	3.8	0.26	0.65
12 wt% PEI/Silica	0.14	0.32	0.46	0.21	0.24	0.18
36 wt% PEI/Silica	0.13	0.28	0.41	0.42	0.48	0.33

Figure S6a revealed the intensity of the negative geminal Si-OH on the PEI/Silica sorbents is less than that of negative Si-OH on silica and the TEPA/Silica sorbents (Figure 4a), confirming that PEI inside the pores prevented full access of benzene to the available Si-OH. The slow responses in the Si-OH intensity profiles during adsorption onto and desorption from the

sorbents shown in Figure S6b confirm the diffusion of benzene is limited by the PEI which filled the pores of the support.

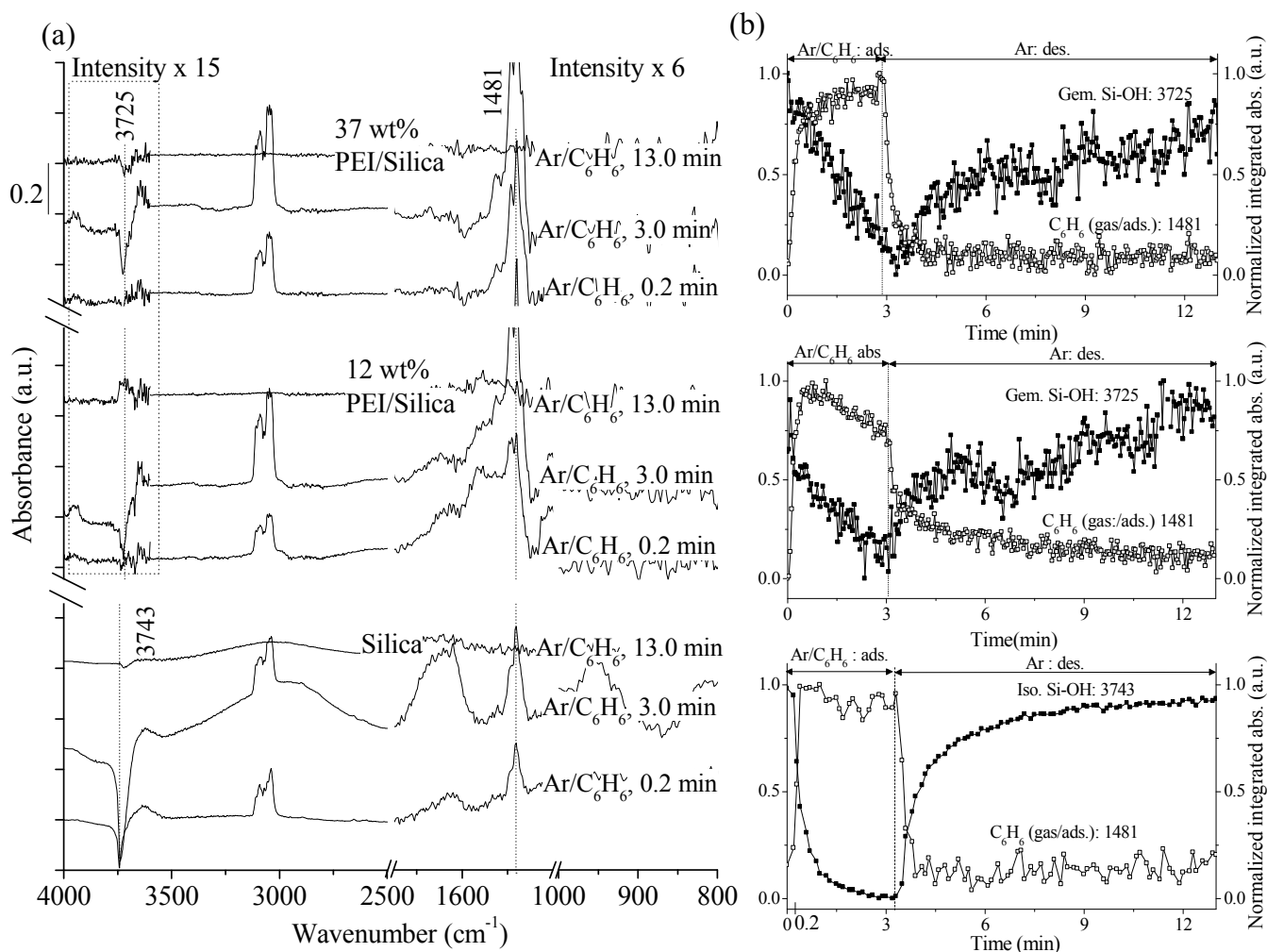


Figure S6. (a) IR absorbance spectra of adsorbed benzene on silica, 12 wt% PEI/Silica, and 36 wt% PEI/Silica at 40 °C after 0.2 and 3.0 in $\text{Ar}/\text{C}_6\text{H}_6$ flow and after 13.0 min in Ar flow, (b) normalized integrated absorbance profiles showing the formation and removal of adsorbed benzene from the isolated and geminal Si-OH groups of silica and the amine sorbents.

Adsorption of CO₂ and benzene onto 36 wt% PEI/Silica shown in Figure S7a produced carbamate/ammonium zwitterions and pairs and carbamic acid similar to adsorption on TEPA/Silica, confirming the formation of the inter-connected network.

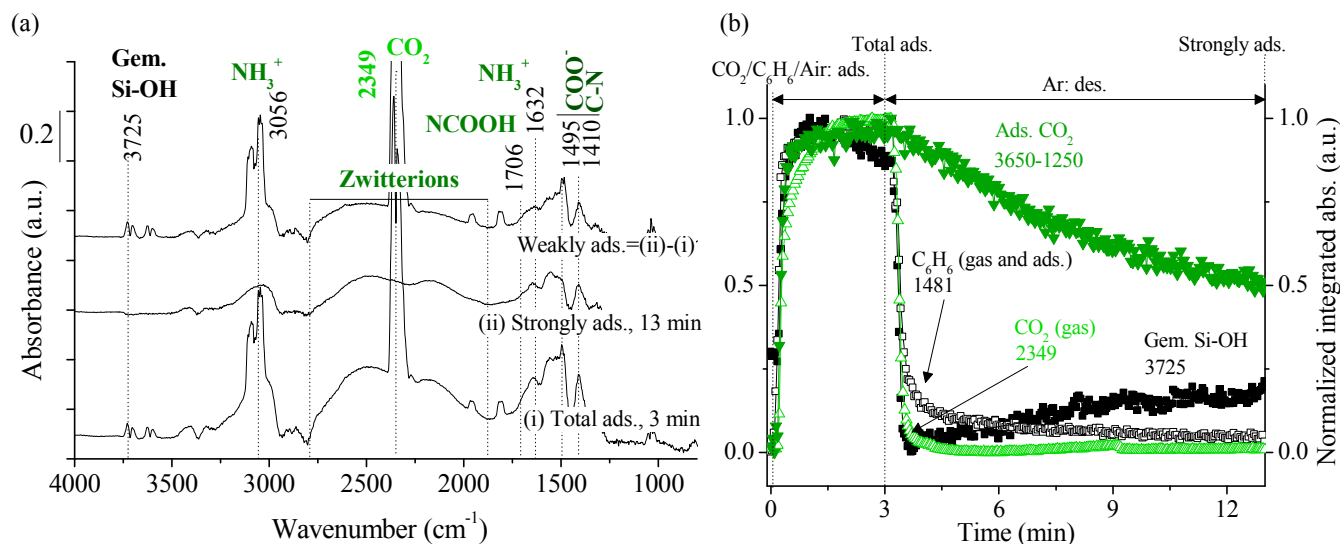


Figure S7. (a) IR absorbance spectra of adsorbed CO₂ and benzene on 36 wt% PEI/Silica at 40 °C in a 10% CO₂/6.8% C₆H₆/air flow after 3 min and in an Ar flow after 13 min, (b) integrated absorbance profiles showing the adsorption and desorption of CO₂ and benzene from the amine sorbent.

The negative geminal Si-OH band was not observed in Figure S7 because of overlapping with CO₂ gas overtones. The intensity profile of adsorbed CO₂ on PEI/Silica in Figure S7b revealed that 85% adsorption capacity was reached after 48 s compared to 15 s for adsorption on TEPA/Silica, shown in Figure 4(a), confirming that impregnated PEI resulted in a greater diffusion limitations through the sorbents pores than impregnated TEPA.

Figure S7(b) shows that purging CO₂ from PEI/Silica by flowing Ar caused fast decay in the adsorbed CO₂ profile (slope=-0.06) compared to slow regeneration in the Si-OH profile (slope=0.02), where the magnified features between 4000-3500 cm⁻¹ of Figure S8 confirm the

presence of the negative Si-OH band. The negative S-OH band emerged as soon as gaseous CO₂ was removed. These results indicate that the removal of adsorbed CO₂ from immobilized, highly viscous PEI or other viscous amine sorbents could occur by “site-hopping” across NH₂ and NH sites (surface diffusion) of amine multi-layers, rather than desorbing into the gas phase and diffusing through or re-adsorbing within the blocked pores. Alternatively, sorbents with higher amine density inside of the pores than on the external particle surface could produce a longer CO₂ diffusion path through the inter-connected network, i.e. more diffusion limitations. However, further evidence is needed to support this.

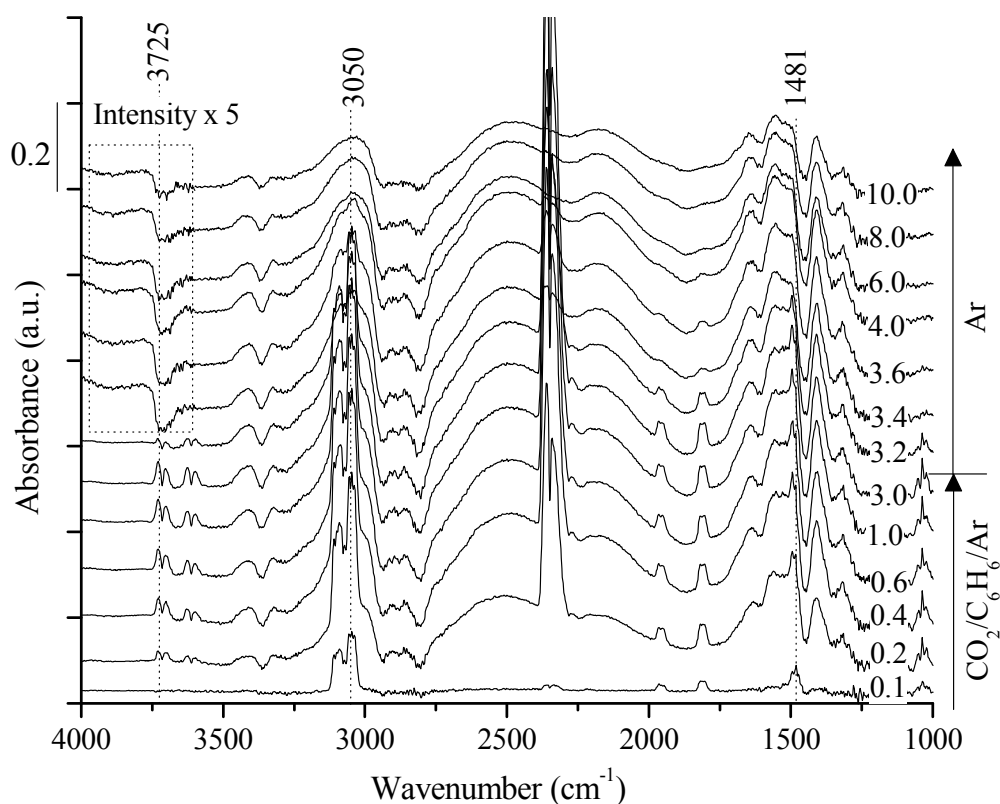


Figure S8. IR absorbance spectra of adsorbed CO₂ and benzene on 36 wt% PEI/Silica at different times during adsorption.